

ON THE PARAMETERS COMPUTATION OF A SINGLE SIDED TRANSVERSE FLUX MOTOR

Henneberger, G.¹ – Viorel, I. A.² – Blissenbach, R.¹ – Popan, A.D.²

¹ Department of Electrical Machines, RWTH Aachen, Schinkelstrasse 4, D-52056 Aachen, Germany.

² Department of Electrical Machines, Technical University of Cluj, C-tin Daicoviciu 15, 3400 Cluj, Romania.

1. INTRODUCTION

The transverse flux (TF) motor represents a relatively new topology of electrical machines. It was first introduced and named by Weh [1] in the late '80s. By now, there have been reports on several variants of TF machines [2]. Basically there are two developments in the fields of TF machine, with or without permanent magnets as excitation. In the both cases the TF machines can be single sided or double sided. The double sided topology is quite complicated therefore the most of the prototypes on which do exist reports are single sided. Since the main feature of the TF machine should be the biggest ratio of the torque with respect to the volume, the TF machine topology with permanent magnets as excitation is the most promising one. The rotor can be built up with surface mounted permanent magnets (flat magnets rotor topology), Fig. 1a, or with permanent magnets inserted in between the flux concentrating poles (concentrating flux rotor topology), Fig 1b, [2]. The flat magnets rotor topology has the advantage of a quite well known technology since some synchronous and DC brushless machines are built up with flat magnets rotor, but the results reported until now lead to the conclusion that the single sided concentrating flux rotor machine topology offers better performances [2, 3, 4].

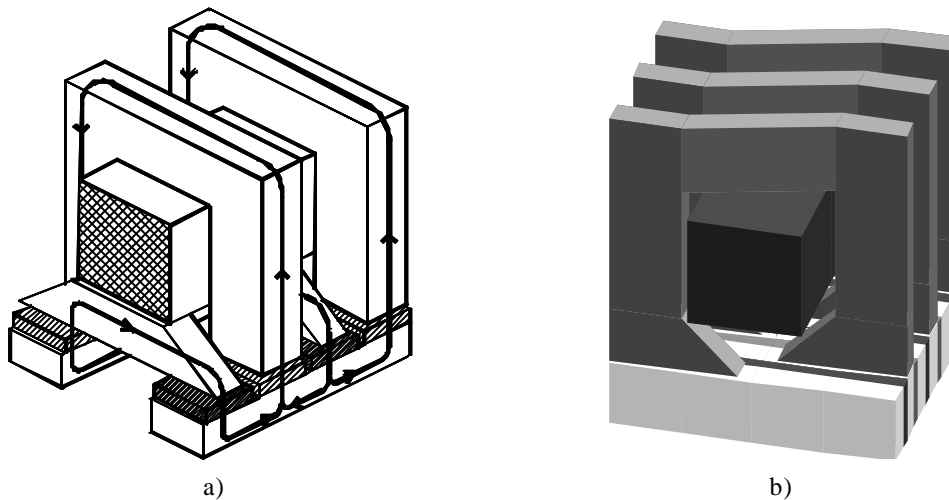


Fig. 1. Single sided TF machine with flat permanent magnets rotor a) and with concentrating flux rotor b)

The TF machine is basically a homopolar one since the stator winding carries current on the circumferential direction and produces a homopolar MMF that is modulated by the stator poles. It results a heteropolar flux density distribution in the air-gap which interact with the heteropolar MMF produced by the permanent magnets' rotor excitation. The TF machine behaves like a synchronous one and the homopolar features allows it to avoid the limitation of the "BiL" principle of force production. The TF machine exhibits a true 3D flux distribution as one can see in Fig 1, where for a better view it is shown only a part of one phase in a linear arrangement. Since the TF machine flux pattern is a quite complicated one with important nonlinearities due to the iron core saturation and permanent magnet operating point change the inductance calculation is not possible by using an analytical exact relation. The flux and consequently the inductance can be computed via a 3D – FEM approach, and this is one of the ways proposed in the paper. In the design – estimation procedure stage there is a need for quite simple relations that allow the inductance calculation. Such relations based on simplified magnetic equivalent circuit to calculate, the magnetizing flux and the corresponding inductance are proposed and the computed values are compared with that obtained via 3D – FEM in the case of different sample TF machines.

2. ANALYTICAL APPROACH

A simple way to compute the phase inductance is by using voltage equation considering that the stator phase current has no component on the d – axis. In this case, since the rotor in both topologies, flat permanent magnets or concentrating flux rotor, exhibits no saliency then the stator phase voltage equations, using phasors, is:

$$\underline{V} = j \cdot X \underline{I} + \underline{E} \quad (1)$$

where V and E are the input phase voltage respectively no load induced EMF in a phase, I is the phase current and X the phase reactance ($X = X_m + X_s$)

The phasor diagram built up based on (1) is given in Fig 2, and the phase reactance comes out as:

$$X = \frac{\sqrt{V^2 - E^2}}{I} \quad (2)$$

Assuming that the input voltage, the induced EMF and the phase current vary sinusoidal, as they do in fact [2, 6], and the frequency f_S is:

$$f_S = n \cdot Q_S \quad (3)$$

where n is the rotor speed and Q_S is the stator polar pieces number, then:

$$L = \frac{\sqrt{V_{\max}^2 - E_{\max}^2}}{I_{\max} \cdot 2p \cdot n \cdot Q_S} \quad (4)$$

Since in the designing – estimation process [2, 5] the input voltage is adopted and the phase current I_{\max} and phase induced EMF E_{\max} are computed the phase inductance can be obtained with (4), the rotor speed value being the rated one. The maximum value of the phase induced EMF, E is given by [2, 5],

$$E_{\max} = N_t \cdot f_{pm} \cdot 2p \cdot n \cdot Q_S^2 \quad (5)$$

where N_t is phase number of turns, f_{pm} is the flux produced by the permanent magnets which was assumed as varying sinusoidal.

In order to determine the flux produced by permanent magnets must be built up a magnetic equivalent circuit (MEC). In the case of flat magnets rotor topology the MEC is quite simple [2, 5] since each polar piece and corresponding "I" core can be considered independent. In the case of concentrating flux rotor topology can be suggested different MEC as one given in [2, 5] for instance, or the one proposed here in Fig 3.

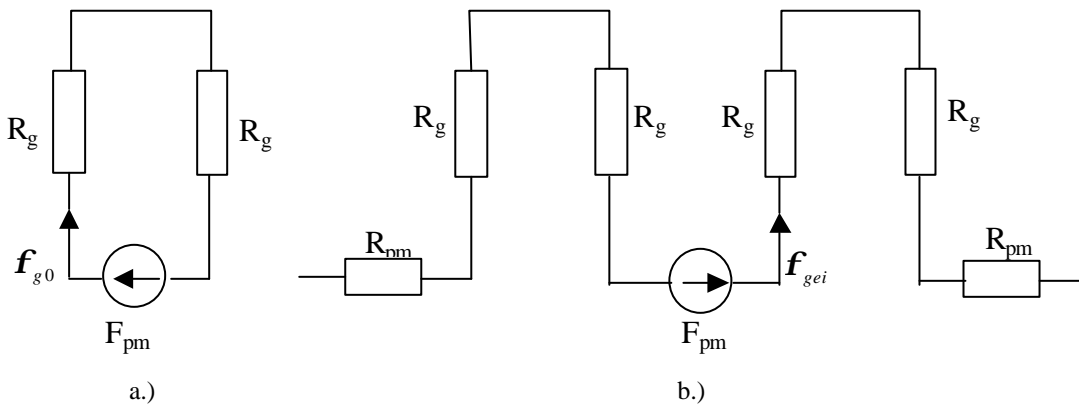


Fig 3. MECs for the TF machine with concentrating flux rotor
 a) polar piece MEC
 b) exterior MEC (circulation flux)

The flux pattern for the concentrated flux rotor topology is shown in an explanatory simplified layout given in Fig 4.

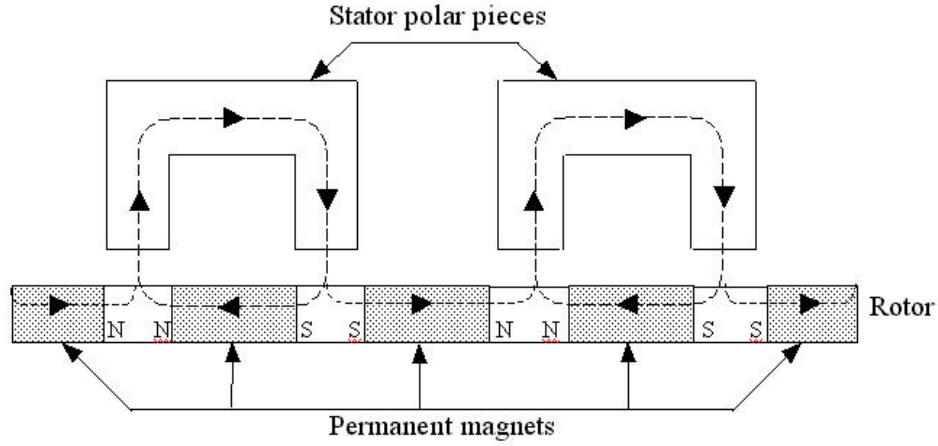


Fig 4. Explanatory simplified layout of the flux pattern for TF machine with concentrating flux rotor.

In the MEC given in Fig 3, as in the MECs developed in [2, 5] the iron core reluctance is neglected against the air-gap and permanent magnet reluctance. Assuming that through a polar piece flow the flux \mathbf{f}_{g0} , Fig 3 a, and all the fluxes \mathbf{f}_{gei} , Fig 3 b, then

$$\mathbf{f}_g = \mathbf{f}_{g0} + \sum_{i=1}^{Q_R/2} \mathbf{f}_{gei} \quad (6)$$

and the corresponding magnetizing inductance is:

$$L_m \cong N_t^2 Q_S \left[\frac{1}{2R_g} + \frac{Q_R}{2} \cdot \frac{1}{\left(\frac{Q_R}{2} - 1\right) \cdot R_{pm} + Q_R R_g} \right] \cdot k_{Lm} \quad (7)$$

and if Q_R is large enough then:

$$L_m \cong N_t^2 Q_S \left[\frac{1}{2R_g} + \frac{1}{R_{pm} + 2R_g} \right] \cdot k_{Lm} \quad (8)$$

which leads to the relation:

$$L_m \cong N_t^2 Q_S \frac{\mathbf{m}_0 A_R}{2g} \left[1 + \frac{\mathbf{m}_{pm}/\mathbf{m}_0}{\frac{h_{pm}}{2g} \cdot \frac{k_{ov}}{k_{fc}} + \frac{\mathbf{m}_{pm}}{\mathbf{m}_0}} \right] \cdot k_{Lm} \quad (9)$$

where A_R is the rotor pole area, g is the air-gap length, \mathbf{m}_{pm} and \mathbf{m}_0 are the permanent magnet and respectively the free air permeability, l_R is the rotor length and k_{ov} , k_{fc} are the overlap factor, respectively the flux concentrating factor [2, 5],

$$k_{ov} = l_{sp}/l_R, \quad k_{fc} = b_{pm}/b_{Rp} \quad (10)$$

the notations being given in Fig 5.

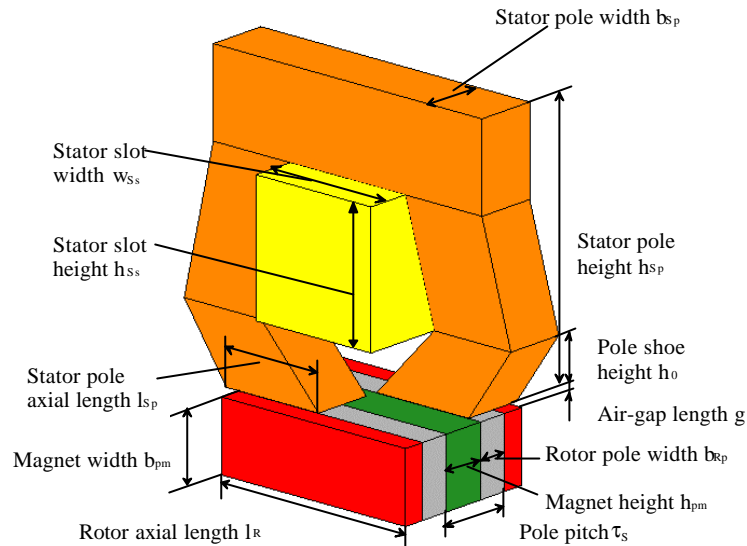


Fig 5. The topology of a TF machine with flux concentrating rotor.

The factor k_{Lm} considers the magnetizing inductance decreasing due to the simplifications made (neglecting permanent magnets leakage and iron core reluctance).
 If the magnetizing inductance is calculated with (9) then the stator phase leakage inductance can be estimated with the relation [6],

$$L_s = \mu_0 p (D_g - g - 2h_0 - h_{ss}) \cdot N_t^2 \left(\frac{h_{ss}}{3w_{ss}} + \frac{h_0}{w_{ss}} \right) \cdot k_{LS} \quad (11)$$

where the D_g is the air-gap diameter and the other notations are given in Fig 5, k_{LS} being a factor which consider the leakage decreasing due to the simplifications made.

3. FINITE ELEMENT APPROACH

The iron parts in the prototype transverse flux machine, whose magnetic circuit is shown in Fig. 6, will be completely made of a soft magnetic composite, which permits the unrestricted construction of the stator cores with respect to the material properties. In order to reduce the flux density values in the stator iron the cross sections of these parts were chosen bigger, as shown in Fig. 6.

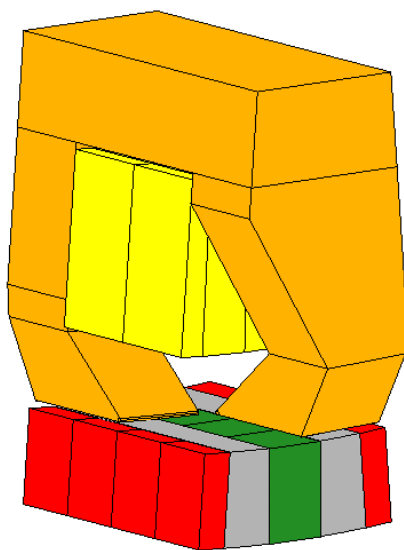


Fig. 6. Magnetic circuit of the prototype transverse flux machine

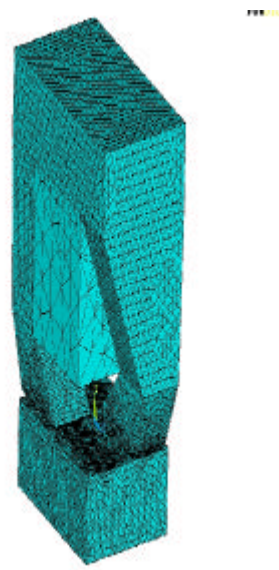


Fig. 7. 3D-FEM mesh of the prototype transverse flux machine

The 3-dimensional FEM mesh of the machine is depicted in Fig. 7 without the surrounding air regions. The complete model consists of 280000 tetrahedral elements and 53000 nodes. For an exact calculation of the forces the air-gap region has to have a very fine meshing.

An example solution for the flux density for the nominal operation is shown in Fig. 8. As it has been expected the flux density in the limbs and the back of the stator core is relatively low and this reduces the iron losses significantly. The stator pole shoes and the rotor flux concentrating pieces near to the air-gap are naturally higher saturated. Also noticeable is the field forcing at the leading edges in both stator and rotor.

The stator inductance results from the modification of the magnetic flux linkage in the winding caused by a changing stator current:

$$L = \frac{d\Psi}{dI} \quad (12)$$

The calculation of the magnetic flux linkage is done with a cross section outside the winding. Because the flux in this region is completely guided in the iron parts, a cross section in the stator core back is absolutely sufficient. As with the FE model only the flux through one pole is computable, the inductance equation is changed to:

$$L = N_i^2 \cdot Q_S \cdot \frac{d\mathbf{f}}{dF} \quad (13)$$

F being the armature MMF. The flux is now calculated with an integration of the flux density over the cross section in the core back:

$$\mathbf{f} = \int B \cdot dA \quad (14)$$

The results obtained are strongly influenced by the stator current and also by the rotor position. In Fig. 9 the stator inductance is shown for a rotor movement of one pole pitch with the armature MMF as parameter. For an electrical angle of 90°, which is the position of minimum excitation flux, the inductance is independent from the stator current, its value being equal to 0.91mH.

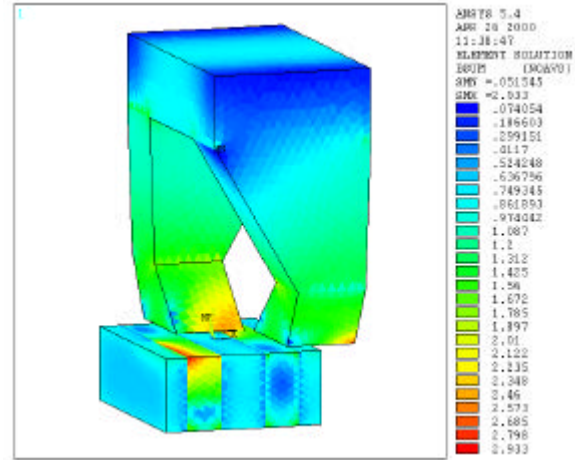


Fig. 8. Flux density for nominal operation of the prototype transverse flux machine

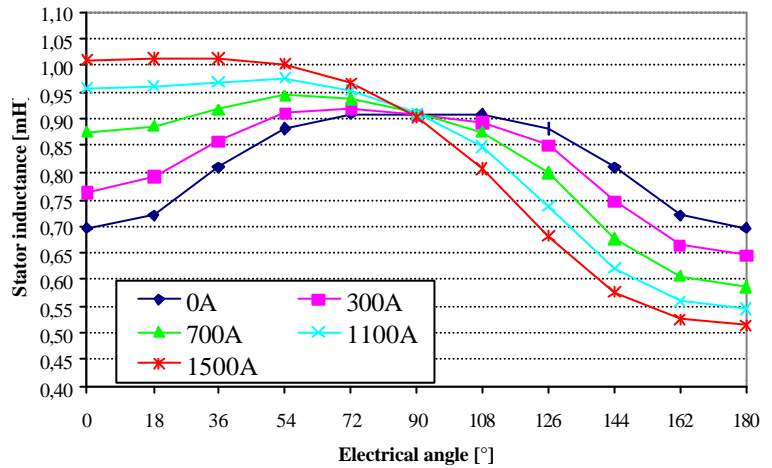


Fig. 9. Stator inductance versus rotor position with armature MMF as parameter

4. COMPUTED RESULTS AND CONCLUSIONS

The prototype TFM considered has the main dimensions and data given in Table 1 and 2 respectively, A_p and A_R being the stator and respectively the rotor pole area [5].

Table 1.

| | | | | | |
|----------|-----------------|------|----------|----|-----|
| A_p | mm ² | 150 | b_{Rp} | mm | 5 |
| A_R | mm ² | 150 | b_{pm} | mm | 10 |
| b_{Sp} | mm | 10 | h_{pm} | mm | 6.5 |
| τ_s | mm | 11.5 | h_0 | mm | 8 |
| l_{Sp} | mm | 15 | h_{Ss} | mm | 20 |
| l_R | mm | 30 | w_{Ss} | mm | 20 |

Table 2

| | |
|---------------------------|-------|
| Rated output power [kW] | 25 |
| Rated phase voltage [V] | 190 |
| Rated phase current [A] | 63 |
| Rated speed [rpm] | 600 |
| Rated torque [Nm] | 400 |
| Number of pole pairs | 40 |
| Air-gap diameter [m] | 0.295 |
| Air-gap length [mm] | 0.8 |
| Stator length [m] | 0.115 |
| Per phase number of turns | 16 |

By using the equation (4) the phase inductance comes out as:

$$L = \frac{\sqrt{(190\text{V} \cdot \sqrt{2})^2 - (185\text{V})^2}}{\sqrt{2} \cdot 63\text{A} \cdot 2p \cdot 600\text{rpm} \cdot 40} = 0.87 \text{ mH} \quad (15)$$

The magnetizing inductance (9) is:

$$L_m = 16^2 \cdot 40 \cdot \frac{4p \cdot 10^{-7} \text{ H/m} \cdot 15 \cdot 10^{-5} \text{ m}^2}{1,6 \cdot 10^{-3} \text{ m}} \cdot \left(1 + \frac{1}{\frac{6,5 \text{ mm}}{1,6 \text{ mm}} \cdot \frac{1}{1,15} \cdot \frac{0,5}{2} + 1} \right) \cdot 0,5 = 0,9235 \text{ mH} \quad (16)$$

where $k_{Lm} = 0.5$, $k_{ov} = 0.5$ and $k_{fc} = 2$.

The leakage inductance, estimated by (11) leads to:

$$L_s = 4p^2 \cdot 10^{-7} \left[0.295 - (0.8 + 16 + 20) \cdot 10^{-3} \right] \cdot 16^2 \left(\frac{20}{60} + \frac{8}{20} \right) \cdot 1.8 = 0.3444 \text{ mH} \quad (17)$$

with $k_{Ls} = 1.8$.

The inductance computed via FEM at no load is 0.91 mH and both values obtained with the analytical relations are quite close to that one. It means that the relations (4) or (9) can be used in an estimation / design procedure with quite good results. The estimate leakage inductance is quite in good agreement with what it should be, the TFM with its homopolar feature having important leakage.

5. REFERENCES

- [1] Weh, H., Jiang, J.: *Berechnungsgrundlagen für Transversal flussmaschinen*, Archiv f. Elektrotechnik, vol. 71, 1988, pp. 187-198.
- [2] Henneberger, G., Viorel, I.A.: *Variable reluctance electrical machines*, Shaker Verlag, Aachen, Germany, 2001.
- [3] Harris, M.R., Pajooman, G.H., Abu Shark, S.M.: *Performance and design optimization of electric motors with heteropolar surface magnets and homopolar windings*, Electr. Power Appl, vol. 143, 1996, no. 6, pp. 429-436.
- [4] Henneberger, G., Blissenbach, R.: *Transverse flux motor with high specific torque and efficiency for direct drive of an electric vehicle*, Proc. of ISATA '99, Vienna, pp.429-436.
- [5] Blissenbach, R., Viorel, I.A., Henneberger, G.: *On the single-sided transverse flux machine design*, to be published.
- [6] Henneberger, G., Viorel, I.A., Blissenbach, R.: *Single-sided transverse flux motors*, Proc. of EPE-PEMC' 2000, vol. 1, pp.19-26.